9-2002

Development of a Finite-Element Stored Grain Ecosystem Model

Michael D. Montross
University of Kentucky, michael.montross@uky.edu

Dirk E. Maier
Purdue University

Kamyar Haghighi
Purdue University

DEVELOPMENT OF A FINITE–ELEMENT STORED GRAIN ECOSYSTEM MODEL

M. D. Montross, D. E. Maier, K. Haghighi

ABSTRACT. *An axisymmetric finite–element model was developed that predicts the heat, mass, and momentum transfer that occurred in upright corrugated steel storage structures due to conduction, diffusion, and natural convection using realistic boundary conditions. Weather data that included hourly total solar radiation, wind speed, ambient temperature, and relative humidity were used to model the temperature, moisture content, dry matter loss, and maize weevil development during storage with no aeration, and with ambient and chilled aeration. Periods of aeration were simulated assuming a uniform airflow rate through the grain mass. Heat and mass balances were used to calculate the temperature and absolute humidity in the headspace and plenum based on solar radiation, wind speed, ambient conditions, air infiltration, convective heat and mass transfer from the grain surface, and permeable boundaries that allowed natural convection currents to cross grain surfaces. A heat balance was used to estimate the wall temperature. The type of weather data in terms of solar radiation and frequency of data appear to be important when predicting the grain temperature, moisture content, dry matter loss, and maize weevil development.*

Keywords. *Modeling, Aeration, Heat transfer, Mass transfer, Storage.*

Insect and mold development are the primary causes of grain deterioration during storage. The development rates are a function of the temperature and moisture distribution within the grain bulk. To accurately predict the level of deterioration during storage, the temperatures and moisture contents need to be correctly estimated. Based on the predicted temperature and moisture contents during storage, estimates of the insect and mold development can be made and the effect of different storage conditions evaluated. The heat and mass transport modes that occur during storage are conduction, diffusion, and natural convection. However, depending on the geometry of the storage structure and material properties of the grain bulk, the effects of natural convection may be negligible (Smith and Sokhansanj, 1990).

A number of models for grain storage have been developed using the finite–difference method that modeled heat conduction during periods of non–aerated storage (Muir et al., 1980; Maier, 1992). Both models included realistic boundary conditions, i.e., the model took into account solar radiation and wind speed. In addition, Maier (1992) included the effects of heat and mass transfer during periods of aerated storage in a model known as the Post–Harvest Aeration and Storage Simulation Tool–Finite Difference Model (PHAST–FDM). Other models have been developed using a finite difference scheme for irregular shapes and mapping the domain to a traditionally spaced grid for solution using simple boundary conditions (Singh et al., 1993) and realistic boundary conditions (Casada and Young, 1994a). Some models have been developed using the control–volume method but have ignored factors like solar radiation and wind speed (Khankari et al., 1995b). One model solved for three–dimensional heat conduction using the finite–element method with realistic boundary conditions (Alagusundaram et al., 1990). However, the models of Alagusundaram et al. (1990), Singh et al. (1993), Casada and Young (1994a), and Khankari et al. (1995b) did not include the effect of forced aeration.

Aeration is an important tool for grain storage management and has to be included if biological aspects of storage modeling are included, such as insect development and dry matter loss. Finally, accurate location–specific weather conditions (dry–bulb temperature, relative humidity, wind speed, snow cover, and solar radiation) are needed for analyzing aeration strategies and boundary effects. To accurately solve for the temperature, moisture content, insect development, and dry matter loss during storage, the boundary conditions need to be realistically modeled. A number of boundary conditions can be applied to finite–element models. Four basic types of boundary conditions are commonly applied to heat and mass transfer problems: prescribed value of dependent variable, convection, flux, and insulated. Directly applying radiation boundary conditions is difficult due to the nonlinear nature of radiation heat transfer (Segerlind, 1984).

Many grain bulks and storage structures are not uniformly shaped, e.g., peaked grain in flat–bottom bins, hopper–

Article was submitted for review in June 2001; approved for publication by Food & Process Engineering Institute of ASAE in May 2002. Presented at the 2000 ASAE Annual Meeting as Paper No. 006043.

Purdue University Agricultural Research Programs Manuscript No. 16422.

The authors are **Michael D. Montross, ASAE Member Engineer**, Assistant Professor, Biosystems and Agricultural Engineering Department, University of Kentucky, Lexington, Kentucky; and Dirk Maier, **ASAE Member Engineer,** Professor, and Kamyar Haghighi, **ASAE Member Engineer,** Professor, Department of Agricultural and Biological Engineering, Purdue University, West Lafayette, Indiana. **Corresponding author:** Dirk E. Maier, 1146 ABE, Purdue University, West Lafayette, IN 47907–1146; phone: 765–494–1175; fax: 765–496–1356; e–mail: maier@purdue.edu.

  ISSN 0001–2351

bottom bins, ground piles, transport vessels, etc. A comprehensive finite–element model would allow for the solution of numerous grain storage structures and would take into account accurate boundary conditions, aeration strategies, estimates of dry matter loss, and development of stored–product insects. In addition, the finite–element method allows for the application of a variety of boundary conditions on irregular–shaped structures without rewriting the computer model (Segerlind, 1984).

Many numerical models of grain storage have used prescribed values of temperature on the boundaries (Khankari et al., 1995b; Singh et al., 1993). Alagusundaram et al. (1990) considered the effects of radiation and wind speed on the wall of a grain bin and assumed that the headspace temperature was equal to the ambient temperature plus 5° C, and the bottom layer of grain was estimated using a Fourier series. Maier (1992) used an energy balance on the headspace, wall, and plenum to estimate the temperature during non–aerated storage in bins equipped with vents and aeration fans. Casada and Young (1994b) used an energy and mass balance to estimate the temperature and humidity above peanuts in a sealed railcar.

The main objective of this research was to develop a numerical simulation model based on the finite–element method to solve the heat, mass, and momentum transfer during aerated and non–aerated storage, determine how accurately boundary conditions needed to be specified, and determine what type of weather data was required for modeling.

Model Development

Governing Equations

For the modeling of non–aerated grain storage, three equations are needed to define the heat, mass, and momentum transfer. Applications of these equations to grain storage can be found in Singh et al. (1993), Casada and Young (1994a), and Khankari et al. (1995b). In many cases, the equations were rearranged to make them non–dimensional or to remove the dependency on the absolute humidity of the air in the mass transfer equation.

The temperature distribution resulting from heat conduction and natural convection while ignoring the effects of heat generation due to fungi and insect development can be written as (Singh et al., 1993; Khankari et al., 1995b):

$$\rho_g c_g \frac{\partial T}{\partial t} + \rho_a c_a u_j \frac{\partial T}{\partial x_j} = \frac{\partial}{\partial x_j}\left(k \frac{\partial T}{\partial x_j}\right) + \rho_g h_{fg} \frac{\partial W_g}{\partial t} \qquad (1)$$

The first term in equation 1 represents the change in enthalpy within the grain bed over time. The second term is the result of heat transfer due to convection. This has to be equal to the heat transfer due to diffusion plus a source term. The source term is the result of water either condensing out of the air onto the grain or evaporating from the grain into the air.

The moisture distribution assuming natural convection and diffusion while neglecting effects due to respiration is (Singh et al., 1993; Khankari et al., 1995b):

$$\rho_g \frac{\partial W_g}{\partial t} + \rho_a u_j \frac{\partial W_a}{\partial x_j} = \frac{\partial}{\partial x_j}\left[\frac{D_v \varepsilon}{\tau} \frac{\partial}{\partial x_j}(\rho_a W_a)\right] \qquad (2)$$

The first term in equation 2 represents the change in moisture content within the grain bed over time. The second term is the effect of natural convection on moisture transfer. The last term is the effect of diffusion on moisture transfer. From equation 2 it can be seen that the change in moisture content of the grain is affected only by the moisture content of the air. An assumption has been made that heat and mass transfer from single–kernel contact can be neglected (Brooker et al., 1992).

Using the assumption by Khankari et al. (1995b) that the air–vapor mixture behaves as an ideal gas, and using the diffusivity of water vapor in air from Thorpe (1981), equation 2 can be rewritten as:

$$\rho_g \frac{\partial W_g}{\partial t} + \frac{u_j}{R_v} \frac{\partial}{\partial x_j}\left(\frac{p_v}{T}\right) = \frac{\partial}{\partial x_j}\left[D_{eff} \frac{\partial}{\partial x_j}\left(\frac{p_v}{T}\right)\right] \qquad (3)$$

Assuming that the vapor pressures of the air and of the grain are equal (Khankari et al., 1995b):

$$\frac{\partial p_v}{\partial x_j} = \left(\left.\frac{\partial p_v}{\partial W_p}\right|_T \frac{\partial W_p}{\partial x_j}\right) + \left(\left.\frac{\partial p_v}{\partial T}\right|_{W_p} \frac{\partial T}{\partial x_j}\right) = \sigma \frac{\partial W_p}{\partial x_j} + \omega \frac{\partial T}{\partial x_j} \qquad (4)$$

then equation 2 can be written as (Khankari et al., 1995b):

$$\rho_g \frac{\partial W}{\partial t} + u_j\left(\frac{\sigma}{R_v T}\right)\frac{\partial W}{\partial x_j} + u_j\left(\frac{\omega}{R_v T}\right)\frac{\partial T}{\partial x_j} = \frac{\partial}{\partial x_j}\left[D_M \frac{\partial W}{\partial x_j}\right] + \frac{\partial}{\partial x_j}\left[D_T \frac{\partial T}{\partial x_j}\right] \qquad (5)$$

where $D_M = \sigma D_{\text{eff}}$ and $D_T = \omega D_{\text{eff}}$.

For different grains, the parameters σ and ω can be determined from the Henderson equilibrium relative humidity equation (Brooker et al., 1992).

The momentum equation in the non–aerated grain storage model can be based on Darcy's law, which describes the natural convection currents that develop as a result of temperature gradients normal to the force of gravity. The buoyancy–driven flows that occur within a grain bulk are sufficiently small so that the pressure gradient is proportional to the velocity gradient. Mathematically this may be expressed as (Thorpe, 1996):

$$\frac{\partial p}{\partial x_j} + \frac{\mu}{K} u + p_a g = 0 \qquad (6)$$

Using Boussinesq's approximation, which assumes that the density of the intergranular air is constant in the heat and mass transfer equations but is variable in the momentum transfer equation, the buoyancy effect is predicted. The momentum equation can be solved using Boussinesq's approximation and the definition of a stream function (Thorpe, 1996). Using the definition of the stream function (ψ), the momentum transfer can be determined (Thorpe, 1996):

$$\frac{\partial^2 \psi}{\partial x^2} + \frac{\partial^2 \psi}{\partial y^2} = -\frac{Kg(\rho_a)_o \beta}{\mu} \frac{\partial T}{\partial x} \qquad (7)$$

Dry matter loss (DML) equations from Stroshine and Yang (1990), Thompson (1972), and Steele et al. (1969) were used to predict fungi growth on shelled corn. Equations from

Throne (1989) were used to simulate the response of the maize weevil (*Sitophilus zeamais* Motschulsky). To estimate the dry matter loss and maize weevil development, the average daily grain temperature and moisture content were required.

Weather Records

In order to simulate the heat, mass, and momentum transfer in grain storage structures, reliable weather data for a site under investigation must be available. Hourly weather data (solar radiation, dry–bulb temperature, wind speed, and relative humidity) for over 30 years is readily available for over 230 U.S. locations (NCDC, 1993). From this data, the heat, mass, and momentum transfer into a storage structure can be estimated based on the solution of the model equations and the appropriate boundary conditions.

Solution Procedure

Equations 1, 5, and 7 are coupled, i.e., there is an interrelation between the temperature, moisture, and momentum equations. A direct analytical solution of these equations is not possible, and therefore an iterative numerical solution procedure has to be used. An iterative procedure similar to Singh et al. (1993), Casada and Young (1994a), and Khankari et al. (1995a) was used:

1. Divide the calculation domain into an appropriate number of elements.
2. Set the grain temperature and moisture content to the appropriate initial values.
3. Update the boundary conditions.
4. Determine the grain material properties based on the most recent estimates of the grain temperature and moisture content.
5. Solve the grain temperature distribution (eq. 1) based on the most recent values of the moisture content and natural convection currents. The heat of vaporization term is handled as a source term during the solution process.
6. Solve the stream function (eq. 7) based on the most recently estimated grain temperature, and calculate the velocities of the natural convection currents from the stream function. The grain temperature gradient is handled as a source term.
7. Solve for the moisture content distribution (eq. 5) using the most recent estimates of the grain temperature and the natural convection currents. Use quadratic elements so that the second derivative of the grain temperature can be easily calculated.
8. Check the accuracy of the solutions, and if the desired convergence has not been reached, then repeat steps 3 through 7. If convergence has been reached, then calculate the dry matter loss, insect development rate, and other relevant end use quality parameters and proceed to the next time step.

The iteration criterion in step 8 was based on comparing the average and maximum change in the calculated values of the grain temperature, moisture content, and stream function after each iteration for each node. An average and maximum error was set for each dependent variable to control the number of iterations. It was determined that two iterations were required to reduce the maximum absolute change in grain temperature, moisture content, and stream function to 0.005° C, 0.001% d.b., and 0.0005 m^2/s, respectively, when hourly time steps were used for most bin sizes. Three iterations reduced the maximum change to 0.00001° C, 0.00005% d.b., and 0.000005 m^2/s for the grain temperature, moisture content, and stream function, respectively. It was decided that the additional accuracy obtained by using three or more iterations was not justified. Therefore, all solutions were performed using two iterations.

The finite–element formulation for the general two–dimensional transport equation is (Comini et al., 1994):

$$\gamma\frac{\partial\phi}{\partial\vartheta}+\beta(v\cdot\nabla\phi+\phi\nabla\cdot v)-\nabla\cdot(\Gamma\nabla\phi)-\dot{s}=0 \tag{8}$$

When the divergence of the velocity field is identically equal to zero, equation 8 for two–dimensional plane or three–dimensional axisymmetric problems can be rewritten as (Comini et al., 1994):

$$\gamma r^{\delta}\frac{\partial\phi}{\partial\vartheta}+\beta r^{\delta}\left(u\frac{\partial\phi}{\partial x}+v\frac{\partial\phi}{\partial y}\right)-\left[\frac{\partial}{\partial x}\left(\Gamma_x r^{\delta}\frac{\partial\phi}{\partial x}\right)+\frac{\partial}{\partial y}\left(\Gamma_y r^{\delta}\frac{\partial\phi}{\partial y}\right)\right]-\dot{s}r^{\delta}=0 \tag{9}$$

This will yield the conventional transport equation in Cartesian coordinates if $\delta = 0$, and the transport equation in axisymmetric coordinates if $\delta = 1$, in which case $x = r$ and $y = z$, $u = v_r$, and $v = v_z$. Three types of boundary conditions can be applied to equation 9:

Part of the boundary (S_ϕ) where the value of ϕ is prescribed (also known as a boundary condition of the first kind or Dirichlet):

$$\phi=\phi_p \tag{10}$$

Part of the boundary (S_{qp}) where the flux is prescribed (also known as a boundary condition of the second kind, or Neumann):

$$\Gamma_x r^{\delta}\frac{\partial\phi}{\partial x}n_x+\Gamma_y r^{\delta}\frac{\partial\phi}{\partial y}n_y+q''_p r^{\delta}=0 \tag{11}$$

Part of the boundary (S_{qc}) where convection takes place (also known as a boundary condition of the third kind):

$$\Gamma_x r^{\delta}\frac{\partial\phi}{\partial x}n_x+\Gamma_y r^{\delta}\frac{\partial\phi}{\partial y}n_y+hr^{\delta}(\phi-\phi_c)=0 \tag{12}$$

A fourth boundary condition is related to equation 11 (also known as an insulated boundary condition):

$$\Gamma_x r^{\delta}\frac{\partial\phi}{\partial x}n_x+\Gamma_y r^{\delta}\frac{\partial\phi}{\partial y}n_y=0 \tag{13}$$

A common approach in the finite–element method is to assume that the shape functions depend on the space coordinates, while the nodal values can be functions of time (Comini et al., 1994):

$$\phi\cong\hat{\phi}=\sum_{i=1}^{n}N_i(x,y)\phi_i(\theta)=N\phi \tag{14}$$

The Galerkin finite–element formulation can be written in matrix form as (Comini et al., 1994):

$$C\dot{\phi}+\overline{K}\phi=\overline{s}+x \tag{15}$$

where

$\underline{C}$ = capacitance matrix

$\overline{K}$ = matrix containing the sum of the homogeneous

contributions

$\bar{S}$ = vector containing the sum of the non–homogeneous contributions

x = vector of unknown nodal reactions arising from boundary conditions of the first kind.

The overall conductance matrix can be written as (Comini et al., 1994):

$$\bar{K}^e = K^e + B^e + A^e + E^e \tag{16}$$

and

$$\bar{s}^e = s^e - p^e - b^e \tag{17}$$

The matrices C^e, K^e, B^e, A^e, and E^e and the vectors s^e, p^e, and b^e for each element are determined by (Comini et al., 1994):

$$C_{ij}^e = \int_{\Omega} N_i \gamma N_j \, d\Omega \tag{18}$$

$$K_{ij}^e = \int_{\Omega} \left(\frac{\partial N_i^e}{\partial x} \Gamma_x r^{\delta} \frac{\partial N_i^e}{\partial x} + \frac{\partial N_i^e}{\partial y} \Gamma_y r^{\delta} \frac{\partial N_i^e}{\partial y} \right) d\Omega \tag{19}$$

$$B_{ij}^e = \int_{S_{qc}^e} N_i^e h r^{\delta} N_j^e \, dS \tag{20}$$

$$A_{ij}^e = \int_{\Omega^e} N_i^e \beta r^{\delta} \left(u \frac{\partial N_j^e}{\partial x} + v \frac{\partial N_j^e}{\partial y} \right) d\Omega \tag{21}$$

$$E_{ij}^e = \int_{\Omega^e} N_i^e \beta r^{\delta} \left(\frac{\partial u}{\partial x} + \frac{\partial v}{\partial y} + \delta \frac{v_r}{r} \right) N_j^e \, d\Omega \tag{22}$$

$$s_i^e = \int_{\Omega^e} N_i^e \dot{s} \, r^{\delta} \, d\Omega \tag{23}$$

$$p_i^e = \int_{S_{qp}^e} N_i^e q_p r^{\delta} \, dS \tag{24}$$

$$b_i^e = -\int_{S_{qc}^e} N_i^e h \phi_c r^{\delta} \, dS \tag{25}$$

If the internal generation ($\dot{s}$) is zero, then all of the element vectors in s^e will be null. If the velocity is zero in the entire domain, then the entries in A^e and E^e are zero, and equation 15 becomes the diffusion equation. In addition, if boundaries of the second kind are specified, then all elements of vector p^e will be zero. Similarly if no boundaries of the third kind are specified, then all elements of matrix B^e and all elements of vector b^e will be zero. If no boundary condition is specified, then the adiabatic boundary condition (eq. 13) is assumed.

To handle the time integration, a two–level algorithm is adopted to solve the system of ordinary differential equations given by equation 15, which produces a matrix equation that is solved (Comini et al., 1994):

$$\left(\frac{1}{\Delta\vartheta} C + \alpha \bar{K} \right) \phi^{n+1} = \left[\frac{1}{\Delta\vartheta} C - (1-\alpha) \bar{K} \right] \phi^n + \bar{s} + \bar{x} \tag{26}$$

where the superscripts n and n+1 refer to the nth and the (n+1)th time steps, respectively. The parameter α can range between 0 and 1. Common finite–difference schemes that can be used to solve equation 26 are:

α = 0.0; explicit Euler method

α = 0.5; Crank–Nicolson

α = 0.6667; Galerkin

α = 1.0; fully implicit.

The Crank–Nicolson integration scheme was used to integrate the equations in time. Overall, the code had approximately 10,000 lines (including comments). The program was written using Fortran 90 and compiled using Digital Visual Fortran 6.0. The program was based on the code from Comini et al. (1994), but was extensively modified, and is known as the Post–Harvest Aeration and Storage Simulation Tool – Finite Element Model (PHAST–FEM)

Boundary Conditions During Non–Aerated Storage

Solar Radiation Components

Relationships from Duffie and Beckman (1991) were used to calculate the solar radiation components on a sloped surface and on vertical walls. The net radiation on a surface has five components: beam, diffuse, sky, earth, and reradiation (Duffie and Beckman, 1991). Total solar radiation (beam plus diffuse) on a horizontal surface can be recorded using a pyranometer. Sky radiation was estimated using a procedure from Maier (1992), and the earth to roof radiation was estimated according to Muir et al. (1980). Reradiation values from ASHRAE (1985) were used. It was assumed that the roof reradiated at 30 W/m^2 and that the wall had zero reradiation. The solution was not stable if reradiation was calculated based on the roof temperature.

Energy Balance

The energy balance for the air in the headspace can be written as the sum of energy fluxes into the headspace air (fig. 1). The heat flux into the headspace is the sum of the convection from the top of the grain surface (q_g), convection from the roof (q_{rf}), air infiltration through the vents (q_{inf}), convection from the exposed wall in the headspace (q_w), and the energy due to natural convection currents that enter and exit the headspace (q_{nc}):

$$\Delta E_{headspace} = q_g + q_{rf} + q_{\inf} + q_w + q_{nc} \tag{27}$$

Equation 27 is a combination of the methods employed by Casada and Young (1994b) and Maier (1992). Casada and Young (1994b) neglected the effects of air infiltration into the headspace because a railcar is sealed. Maier (1992) assumed that natural convection within a grain bin was minimal and therefore neglected the heat transfer from natural convection currents entering into the headspace. The air infiltration rate was estimated using data from ASHRAE (1985) based on the design infiltration rate of 0.67 volumes per hour into an attic. It was determined that one roof and wall temperature would not produce realistic headspace temperatures. Therefore, the roof and wall were divided into four areas. Each area was assumed to face due south, west, north, or east and modeled as a flat–plate solar collector using procedures given by Duffie and Beckman (1991). It was assumed that heat conduction through the roof and wall were one–dimensional. Therefore, equation 27 can be expressed as:

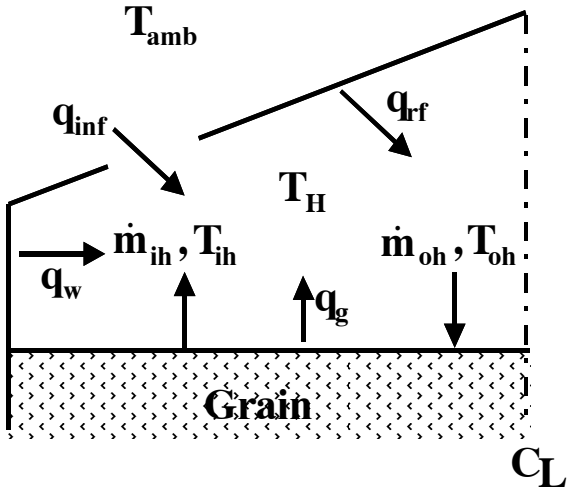

Figure 1. Energy balance on the headspace air.

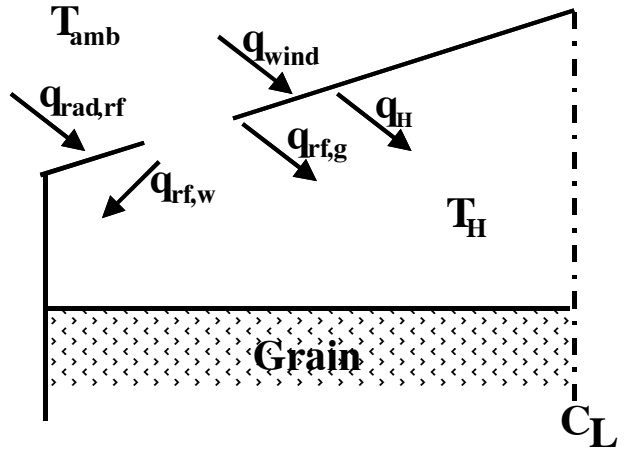

Figure 2. Energy balance on the roof of the headspace.

$$(\rho c)_a V_H \frac{dT_H}{dt} = h_g A_g (T_g - T_H) + \sum_{i=1}^{4} h_{ri} A_{rf} (T_{rf,i} - T_H)$$
$$+ \frac{c_a V_H X_H}{\upsilon} (T_{amb} - T_H) + \sum_{i=1}^{4} h_{wi} A_w (T_{w,i} - T_H)$$
$$+ \dot{m}_{iH} c_a (T_{iH} - T_H) - \dot{m}_{oH} c_a (T_{oH} - T_H) \quad (28)$$

It was assumed that the headspace temperature could be represented as one temperature due to turbulence. Casada and Young (1994b) calculated a Rayleigh number considerably greater than 1.4×10^7 during periods of solar heating, which according to Fraikin et al. (1980) was the point at which turbulent flow would occur in a square enclosure. Turbulent flow would tend to increase the mixing of the air, allowing the use of one average temperature to describe the headspace.

The change in energy of the roof (fig. 2) can be written as the sum of heat flows into and out of the roof (Casada and Young, 1994b; Maier, 1992). The change in energy of the roof is equal to the heat flow due to the wind (q_{wind}), convection from the roof into the headspace (q_H), solar radiation on the roof ($q_{rad,rf}$), reradiation from the roof (q_{re}), radiation between the roof and grain surface ($q_{rf,g}$), and radiation between the roof and wall ($q_{rf,w}$):

$$\Delta E_{rf} = q_{wind} + q_H + q_{rad,rf} + q_{rf,g} + q_{rf,w} + q_{re} \quad (29)$$

The energy balance on each section of roof can be rewritten as:

$$(\rho c)_{rf} t_{rf} \frac{dT_{rf,i}}{dt} = h_{ro}(T_{amb} - T_{rf,i}) + h_{ri}(T_H - T_{rf,i})$$
$$+ \alpha G_{T,i} + \varepsilon G_{s,i} + \varepsilon G_{e,i} - \varepsilon G_{r,i} + SF_{rf,g} \varepsilon_{ri} \sigma \left(T_H^4 - T_{rf}^4 \right)$$
$$+ SF_{rf,w} \varepsilon_{ri} \sigma \left(T_w^4 - T_{rf}^4 \right) \quad (30)$$

where the subscript i refers to each section of roof. A value of 0.5 was used for all the shape factors, similar to Muir et al. (1980). However, the radiation from the earth ($G_{e,i}$) is zero because the roof does not see the earth. Convective heat transfer coefficients due to the wind were assumed not to vary with direction and were taken from Finnigan and Longstaff (1982). The energy balance for each section of wall is similar to the roof, except that the wall does not see the sky and there is radiation exchange between the earth and wall. Nine simultaneous first–order ordinary differential equations (ODEs) (one for the headspace, four for the roof, and four for the wall in the headspace) were numerically solved using an adaptive Runge–Kutta procedure.

Similar energy balances were developed for the plenum temperature and for the wall that was in contact with the grain mass. A system of five ODEs for the plenum boundary and one ODE for the wall in contact with grain were solved using a Runge–Kutta procedure. The derivation of the plenum and wall in contact with the grain boundary conditions is given by Montross (1999). Based on the headspace, plenum, and wall temperatures, convective heat transfer was assumed to occur with the grain surfaces.

Moisture Balance

The humidity ratio of the headspace air was calculated using a mass balance similar to Casada and Young (1994b). The change in humidity ratio of the headspace air is equal to the mass flux due to convection from the top of the grain surface (j_g), mass flux due to the natural convection currents entering and exiting the headspace (j_{nc}), and mass flux due to ventilation with the ambient conditions (j_{vth}):

$$\Delta W_H = j_g + j_{nc} + j_{vth} \quad (31)$$

It was assumed that no mass transfer occurred across the wall or roof surfaces. Rewriting equation 31 gives:

$$\rho_a V_H \frac{d\gamma_H}{dt} = h_g A_g (\gamma_g - \gamma_H) + \dot{m}_{in} (\gamma_{iH} - \gamma_H)$$
$$- \dot{m}_{out} (\gamma_{oH} - \gamma_H) + \dot{m}_{vth} (\gamma_{amb} - \gamma_H) \quad (32)$$

A similar mass balance was developed for the plenum air (Montross, 1999). One ODE for the plenum and headspace absolute humidities was solved using a Runge–Kutta procedure.

Stream Function

For impermeable boundaries, a value of zero is specified for the stream function (Thorpe, 1996). Burns and Stewart (1992) investigated the natural convection currents that occurred in a concentric annulus with permeable boundaries.

To accomplish a permeable boundary, a zero pressure boundary condition was applied to the grain surfaces in contact with the headspace air and plenum air:

$$\frac{\partial \Psi}{\partial y} = 0 \qquad (33)$$

Possible Condensation Conditions

Solution of equation 32 can result in relative humidities greater than 100%. A number of processes can occur within the headspace that would limit the relative humidity to 99%. One location where water vapor condenses in a bin is on the underside of the roof. From there, three things can happen: the condensate can drip onto the grain, it can run down the roof through the eave and drip outside of the bin, or it can stay on the roof until the headspace relative humidity decreases and the condensate evaporates back into the headspace air. Another location where water vapor condenses in a bin is onto the grain surface itself.

Although condensation and frost conditions are known to occur at times, the exact processes occurring in a grain bin during condensation have not been described in the literature. As a result, when the simulation model predicted a relative humidity over 100%, the absolute humidity was adjusted to give a relative humidity of 99%. The condensation was assumed to occur as drops on the underside of the roof, which do not form a film. It was also assumed that the heat transfer coefficient was not affected (Holman, 1990). The underside of the roof represented storage for the condensate until it could be evaporated back into the headspace air. The roof temperature changes slightly due to evaporation or condensation and was estimated by multiplying the mass of water undergoing a phase change times the heat of vaporization of water vapor.

Modifications During Aerated Storage

During periods of aeration, the natural convection equation was ignored. Air velocities based on the aeration flow rate were specified at each node and were assumed to be uniform. The air velocity in the plenum was calculated based on a fan curve and Shedd's curves (*ASAE Standards*, 1997). However, the actual air velocity within the grain bulk is considerably greater due to the porous nature of the grain bulk. The heat and mass transfer equations are based on the interstitial velocities within the grain bulk. The apparent velocity in the plenum can be converted to the interstitial velocity through the grain bulk by dividing by the porosity (Brooker et al., 1992).

The boundary conditions in the headspace and plenum are calculated differently during periods of aeration. The temperature and relative humidity in the plenum were set equal to the ambient conditions plus the effect of fan pre–warming due to air compression and heat from the motor. It was assumed that the grain temperature of the bottom nodes at the plenum interface was at thermal equilibrium with the plenum air after each time step. The moisture content of the bottom nodes at the plenum interface was calculated using the thin–layer drying and rewetting equations from Misra and Brooker (1980). The model was then solved using fixed values of temperature and moisture content as the plenum boundary condition. The energy and mass balance for the headspace air was modified to prevent air infiltration through the vents. In addition, the heat and mass transfer from natural convection between the headspace air and grain surface was neglected.

Model Evaluation

Effect of Realistic Boundary Conditions

Fully instrumented corrugated steel bins (Chore–Time Brock, Inc., Milford, Ind.) with a diameter of 2.74 m and an eave height of 3.05 m with a maximum capacity of 11.7 t are available at the Purdue University Post Harvest Education and Research Center (PHERC) pilot bin facility located at the Agronomy Research Center, West Lafayette, Indiana. Figure 3 shows the solar radiation on a flat surface recorded

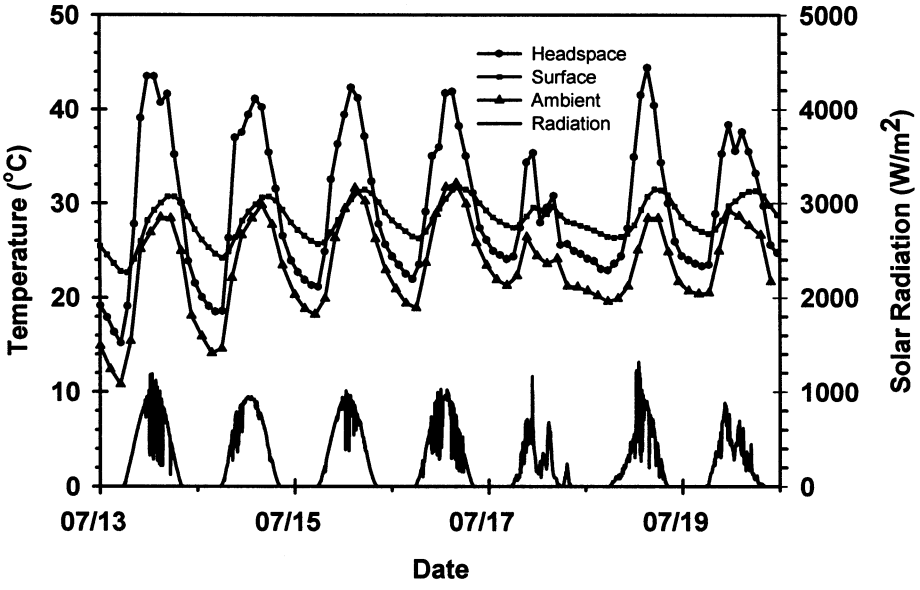

Figure 3. Measured solar radiation and ambient, corn surface, and headspace temperatures in a non–aerated bin during the summer of 1999.

using a silicon pyranometer, the temperature at the grain surface (1 to 3 kernels deep), the air temperature at the midpoint of the headspace, and the ambient temperature in a non–aerated pilot bin during a typical period in 1999. During periods of high solar radiation, the headspace temperature reached almost 45° C, while during periods of intermittent solar radiation (17 July) the headspace temperature reached only 35° C. The temperature of the grain surface fluctuated sinusoidally between 22° C and 31° C.

Overall, from 1 June to 1 September 1999, the average ambient, grain surface, and headspace temperatures during non–aerated storage were 21.7° C, 26.8° C, and 28.2° C, respectively. In a bin with automatic ambient aeration, the average grain surface and headspace temperatures were 24.5° C and 27.7° C, respectively. This indicates the potential effect of solar radiation on the predicted heat transfer during storage between the grain surface and the headspace air. Similar data and conclusions were found for the wall and plenum of bins with no aeration, ambient, and chilled aeration (Montross, 1999).

Figure 4 shows the roof and dew point temperature measured in the headspace of a typical bin during early spring of 1999. The dew point temperature was calculated from the measured relative humidity and air temperature in the headspace, and the roof temperature was measured with a thermocouple mounted to the underside of the roof. Numerous periods were determined when condensation occurred. Condensation was visibly observed on several occasions, but the amount of water accumulation during condensation was not measured. However, these observations and measurements confirm that condensation occurs during storage and should be modeled.

Similar results with respect to the importance of realistic boundary conditions were found for the relative humidity difference between the headspace and ambient air. From 1 June to 1 September 1999, the average ambient relative humidity was 81%. The average relative humidities in the headspace of a non–aerated and ambient aerated bin were 58% and 55%, respectively. Properly estimating the roof temperature, headspace relative humidity, and headspace temperature are important when evaluating aeration strategies and possible condensation conditions.

Importance of Weather Data

Most researchers have used daily average temperature values as inputs to their storage models, and many have neglected solar radiation and wind speed. The PHAST–FEM model was used to simulate the effect of four types of weather data from Indianapolis, Indiana, using available weather data between 1 May and 1 October 1990. A total of four simulations were run to demonstrate the differences in the predicted average corn temperature in a 9 m diameter bin filled to a depth of 6 m with corn initially at a uniform temperature and moisture content of 15° C and 15% w.b., respectively, on 1 May. It was assumed that an initial population of one pair of adult maize weevils per tonne was in the grain mass on 1 May. Maize weevil populations were predicted based on the average grain temperature and moisture content in the bin at the end of each day. Aeration was simulated assuming upward aeration at an airflow rate of 0.1 $m^3\ min^{-1}\ t^{-1}$ when the ambient air temperature was 15° C or colder. Two simulations were run using hourly weather data: one simulation included the effects of solar radiation and wind speed (realistic conditions), and the other simulation did not (unrealistic conditions). Two additional simulations used daily averaged weather data: one simulation included the effects of solar radiation and wind speed (realistic conditions), and the other simulation did not (unrealistic conditions).

Table 1 summarizes the final predicted grain conditions (on 1 October 1990) after five months of summer storage. The periphery region represents the volume of corn within 1.0 m of the headspace, wall, and plenum. Hourly weather data that included solar radiation and wind speed had an average final corn temperature of 14.8° C, which was between 1.4° C and 2.0° C warmer than the simulations with unrealistic boundary conditions on 1 October 1990. A major difference was in the periphery region, which was heavily

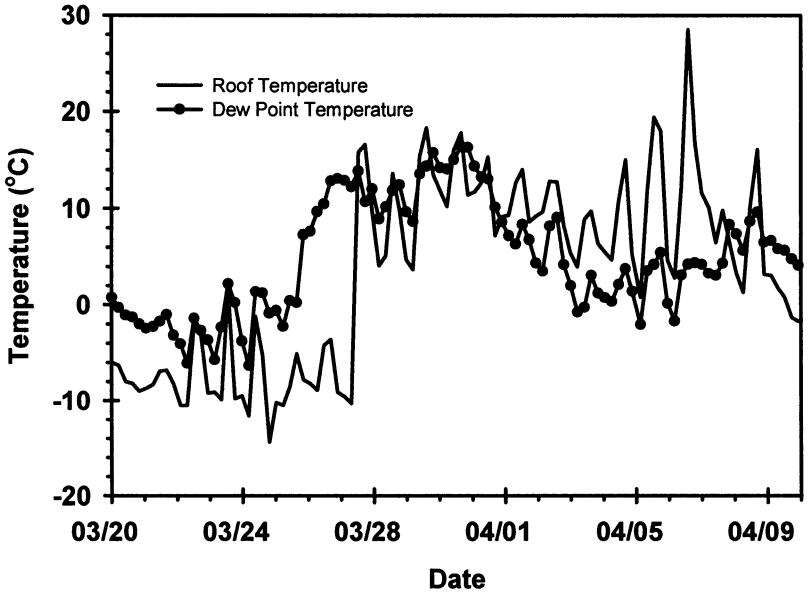

Figure 4. Roof and dew point temperatures in the headspace showing periods of condensation in a bin during the spring of 1999.

Table 1. Effect of weather data on final predicted conditions[a] after storage of corn initially at 15° C and 15% w.b. with intermittent aeration between 1 May and 1 October 1990.

	Hourly Data		Daily Data	
Condition	Including solar radiation and wind speed	Neglecting solar radiation and wind speed	Including solar radiation and wind speed	Neglecting solar radiation and wind speed
Average bin temperature (°C)[a]	14.8	12.8	13.4	13.2
Average periphery grain temperature (°C)[a,b]	20.2	13.9	14.6	14.2
Average bin dry matter loss (%)[a]	0.36	0.15	0.20	0.17
Average periphery dry matter loss (%)[a,b]	0.87	0.21	0.31	0.23
Average grain moisture content (%)[a]	14.3	15.0	14.8	14.8
Average periphery moisture content (%)[a,b]	13.0	15.1	14.8	14.8
Fan runtime (h)[c]	680	680	504	504
Maize weevil population (adults/t)[a,d]	77.2	24.1	31.9	24.1

[a] Values are based on averages on 1 October 1990.
[b] The periphery volume of the bin is defined as the corn within 1 m of the wall, headspace, and plenum.
[c] Fan operation occurred whenever the ambient temperature was 15° C or cooler.
[d] Initial maize weevil population was 1 adult pair per tonne.

influenced by solar radiation. The average periphery temperature at the end of the summer was 20.2° C, which was between 5.6° C and 6.3° C warmer than the simulations with unrealistic boundary conditions. The warmer conditions in the periphery increased the predicted DML and maize weevil development. The predicted DML with hourly weather data, including solar radiation and wind speed, was between 80% and 140% greater than the predictions with unrealistic boundary conditions.

Figure 5 presents the estimated average bin temperature during the summer storage period using the four types of weather data. During the five–month storage period, the average simulated corn temperature was 17.7° C, with a maximum temperature of 22.3° C, when hourly temperature data, solar radiation, and wind speed were included. When solar radiation and wind speed were neglected, the simulated average corn temperature was 14.9° C, with a maximum of 17.4° C, for hourly temperature data. When the weather data was converted to a daily average temperature and solar radiation and wind speed were neglected, the average corn temperature was 14.9° C, with a maximum of 17.0° C. When daily weather data including solar radiation and wind speed were used, the average corn temperature was 15.3° C, with a maximum temperature of 17.6° C. The temperature differences were more significant near the walls and headspace (not shown). The average bin temperature when solar radiation and wind speed were considered was 2.8° C higher compared to the simulation neglecting solar radiation and wind speed. However, in the region within 1.0 m of the wall and headspace, the average temperature was 7.0° C warmer.

Hourly time steps are critical when the effectiveness of aeration controllers is being investigated. When daily averaged weather data were used, the total runtime during the summer was 504 h compared to 680 h (table 1) with hourly

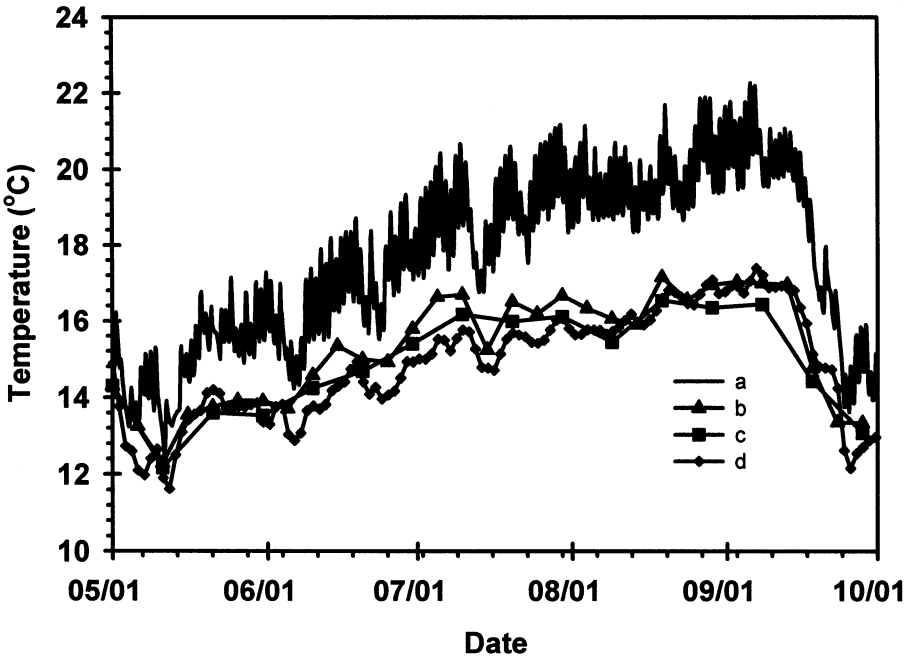

Figure 5. Simulated average corn temperature in an aerated bin: (a) using hourly ambient temperature, wind speed, and solar radiation; (b) using daily average temperature, wind speed, and solar radiation; (c) using daily average temperature and neglecting wind speed and solar radiation; and (d) using hourly ambient temperature and neglecting wind speed and solar radiation.

weather data. In addition, the type of weather data used in the simulation affected the average predicted moisture content. When average daily weather conditions with or without solar radiation and wind speed were used, the average predicted moisture content on 1 October 1990 was 14.8% (table 1). When hourly weather data were used, the average bin moisture contents were 15.0% and 14.3% w.b. when solar radiation and wind speed were neglected and included, respectively. Including solar radiation decreased the predicted average moisture content because solar radiation increased the grain temperature, which in turn increased the moisture loss, especially along the sidewalls, whenever the aeration fan was operated.

When dry matter loss was estimated using the four different weather data sets, large differences occurred (fig. 6). When hourly temperature, solar radiation, and wind speed data were included, the average dry matter loss at the end of the storage season for the entire bin was 0.36%. However, when hourly temperatures were used and solar radiation and wind speed were neglected, the predicted dry matter loss was only 0.15%. The total maize weevil population at the end of the storage period was 24.1 adults/t when no radiation or wind speed was simulated for hourly and daily averaged weather data. However, when solar radiation and wind speed were included, the predicted populations were 77.2 and 31.9 adults/t when hourly and daily averaged weather data were used, respectively. Similar results were found with non–aerated and other ambient and chilled aeration strategies (not shown).

Conclusions

A finite–element model was developed to simulate the heat and mass transfer during aerated and non–aerated storage due to diffusion, conduction, and natural convection. Aeration, dry matter loss, and maize weevil development were included in the new model. The following conclusions were drawn with respect to the required refinement of the PHAST–FEM model:

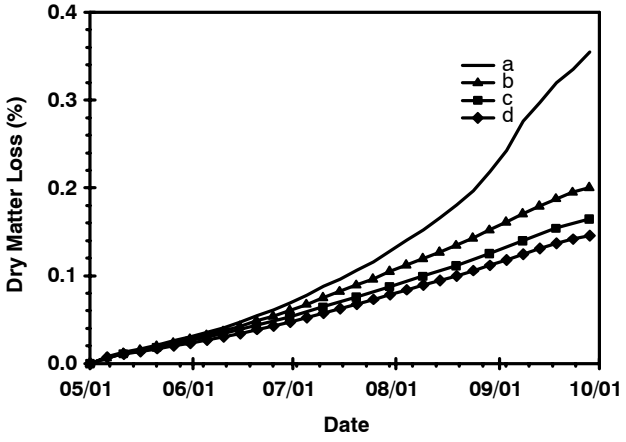

Figure 6. Simulated average corn dry matter loss in an aerated bin: (a) using hourly ambient temperature, wind speed, and solar radiation; (b) using daily average temperature, wind speed, and solar radiation; (c) using daily average temperature and neglecting wind speed and solar radiation; and (d) using hourly ambient temperature and neglecting wind speed and solar radiation.

- There were significant differences between the headspace, grain surface, and ambient temperatures during aerated and non–aerated storage. This indicated the need to model the boundaries in the headspace, plenum, and around the wall to accurately model the heat and mass transfer into a grain bulk during storage.
- Solar radiation had a large impact on predicted grain temperatures, moisture contents, dry matter loss, and maize weevil development during storage. Neglecting solar radiation resulted in a predicted average grain temperature that was 2° C cooler, and 7° C cooler in the periphery regions of a bin, after five months of storage.
- The time step used during simulation was important to accurately model the heat and mass transfer near the boundaries. Hourly time steps predicted fan operation of 680 h compared to 504 h for daily averaged weather data, which is an important difference when aeration strategies for summer storage and biological aspects of storage were investigated.

Acknowledgements

The financial support through USDA–NRI Competitive Grant 96–35313–3728 and by General Mills Inc., Minneapolis, Minnesota, in the form of a three–year General Mills IPM Fellowship is acknowledged.

References

Alagusundaram, K., D. S. Jayas, N. D. G. White, and W. E. Muir. 1990. Three–dimensional finite element heat transfer model of temperature distribution in grain storage bins. *Trans. ASAE* 33(2): 577–584.

ASAE Standards. 1997. ASAE D272.3: Resistance to airflow of grains, seeds, other agricultural products, and perforated metal sheets. St. Joseph, Mich.: ASAE.

ASHRAE. 1985. *ASHRAE Handbook*. Atlanta, Ga.: ASHRAE.

Brooker, D. B., F. W. Bakker–Arkema, and C. W. Hall. 1992. *Drying and Storage of Grains and Oilseeds*. New York, N.Y.: Van Nostrand Reinhold.

Burns, A. S., and W. E. Stewart, Jr. 1992. Convection in heat–generating porous media in a concentric annulus with a permeable outer boundary. *Int. Comm. Heat Mass Transfer* 19(1): 127–136.

Casada, M. E., and J. H. Young. 1994a. Model for heat and moisture transfer in arbitrarily shaped two–dimensional porous media. *Trans. ASAE* 37(6): 1927–1938.

_____. 1994b. Heat and moisture transfer during transportation of shelled peanuts. *Trans. ASAE* 37(6): 1939–1946.

Comini, G., S. D. Giudice, and C. Nonino. 1994. *Finite Element Analysis in Heat Transfer: Basic Formulation and Linear Problems.* Washington, D.C.: Taylor and Francis.

Duffie, J. A., and W. A. Beckman. 1991. *Solar Engineering of Thermal Processes.* New York, N.Y.: John Wiley and Sons.

Finnigan, J. J., and R. A. Longstaff. 1982. A wind–tunnel model study of forced convective heat transfer from cylindrical grain storage bins. *J. Wind Eng. and Industrial Aerodynamics* 10(2): 191–211.

Fraikin, M. P., J. J. Portier, and C. J. Fraikin. 1980. Application of a k–e turbulence model to an enclosed buoyancy–driven recirculating flow. ASME Paper No. 80–HT–68. New York, N.Y.: ASME.

Holman, J. P. 1990. *Heat Transfer.* New York, N.Y.: McGraw–Hill.

Khankari, K. K., S. V. Patankar, and R. V. Morey. 1995a. A mathematical model for natural convection moisture migration in stored grain. *Trans. ASAE* 38(6): 1777–1787.

Khankari, K. K., R. V. Morey, and S. V. Patankar. 1995b. Application of a numerical model for prediction of moisture migration in stored grain. *Trans. ASAE* 38(6): 1789–1804.
Maier, D. E. 1992. The chilled aeration and storage of cereal grains. Unpublished PhD diss. East Lansing, Mich.: Michigan State University.
Misra, M. K., and D. B. Brooker. 1980. Thin–layer drying and rewetting equations for shelled yellow corn. *Trans. ASAE* 23(5): 1254–1260.
Montross, M. D. 1999. Finite–element modeling of stored grain ecosystems and alternative pest–control techniques. Unpublished PhD diss. West Lafayette, Ind.: Purdue University.
Muir, W. E., B. M. Fraser, and R. N. Sinha. 1980. Simulation model of two–dimensional heat transfer in controlled–atmosphere grain bins. In *Controlled Atmosphere Storage of Grains*, 385–397. J. Shejbal, ed. Amsterdam, The Netherlands: Elsevier Scientific Publishing.
NCDC. 1993. Solar and Meteorological Surface Observation Network. Asheville, N.C.: National Climatic Data Center and National Renewable Energy Laboratory.
Segerlind, L. J. 1984. *Applied Finite Element Analysis*. New York, N.Y.: John Wiley and Sons.
Singh, A. K., E. Leonardi, and G. R. Thorpe. 1993. A solution procedure for the equations that govern three–dimensional free convection in bulk stored grains. *Trans. ASAE* 36(4): 1159–1173.
Smith, E. A., and S. Sokhansanj. 1990. Moisture transport caused by natural convection in grain stores. *J. Agric. Eng. Res.* 47(1): 23–34.
Steele, J. L., R. A. Saul, and W. V. Hukill. 1969. Deterioration of shelled corn as measured by carbon dioxide production. *Trans. ASAE* 12(5): 685–689.
Stroshine, R. L., and X. Yang. 1990. Effects of hybrid and grain damage on estimated dry matter loss for high–moisture shelled corn. *Trans. ASAE* 33(4): 1291–1298.
Thorpe, G. R. 1981. Moisture diffusion through bulk grain. *J. Stored Prod. Res.* 17(1): 39–42.
_____. 1996. Modeling moisture migration in stored grains. In *Grain Drying in Asia*, 99–122. B. R. Champ, E. Highley, and G. I. Johnson, eds. Proceedings of an international conference held at the FAO Regional Office for Asia and the Pacific. Bangkok, Thailand. 17–20 October 1995.
Thompson, T. L. 1972. Temporary storage of high–moisture shelled corn using continuous aeration. *Trans. ASAE* 15(2): 333–337.
Throne, J. E. 1989. Effects of noncatastrophic control technologies that alter life history parameters on insect population growth: A simulation study. *Environ. Entom.* 18(6): 1050–1055.

NOMENCLATURE

c = specific heat (J kg^{-1} K^{-1})
h = convective heat or mass transfer coefficient (W m^{-2} K^{-1}; kg m^{-2} s^{-1})
h_{fg} = latent heat of vaporization (J/kg)
j = mass flow (kg/s)
k = thermal conductivity (W m^{-1} K^{-1})
g = acceleration due to gravity (m/s^2)
$\dot{m}$ = mass flow rate (kg/s)
p = pressure (Pa)
q = heat flow (W/m^2)
t = time (s), thickness (m)
u = velocity (m^3 m^{-2} s^{-1})
x_j = tensor notation for direction (m)
A = area (m^2)
$D_{\text{eff}} = \dfrac{D_v \varepsilon}{R_v \tau}$
D_v = diffusivity of water vapor in air (m^2/s)
K = permeability (–)
G = solar irradiance (W/m^2)
R_v = water vapor gas constant (461.52 J kg^{-1} K^{-1})
$SF_{rf,g}$ = shape factor between the roof and grain surface
$SF_{w,g}$ = shape factor between the wall and grain surface
T = temperature (K)
V = volume (m^3)
W = moisture content (decimal dry basis, kg of water per kg of dry air)
X = infiltration rate (volumes/s)

SUBSCRIPTS

a = air
amb = ambient
e = earth
g = grain, grain surface
iH = into headspace
inf = infiltration
nc = natural convection currents
oH = out of headspace
r = reradiation
rad,rf = radiation on the roof
rf = roof
ri = inside of roof
ro = outside of roof
s = sky
v = vapor
w = wall
wi = inside of wall
H = headspace
T = total

GREEK SYMBOLS

α = absorptivity (–)
β = coefficient of thermal expansion (K^{-1})
ε = porosity (m^3 of air/m^3 of grain), emissivity (–)
γ = humidity ratio (kg H_2O/kg dry air)
μ = viscosity of air (kg m^{-1} s^{-1})
ρ = density (kg/m^3)
$(\rho_\alpha)_o$ = air density at reference temperature (kg/m^3)
σ = change in partial pressure due to moisture content at constant temperature (Pa)
τ = tortuosity factor (–)
υ = specific volume (m^3/kg)
ω = change in partial pressure due to temperature at constant moisture content (Pa/K)
ψ = stream function (m^2/s)